

# Electronic Structure of Molybdenene

Ashkan Shekaari<sup>1,\*</sup>

<sup>1</sup>*Department of Physics, K. N. Toosi University of Technology, Tehran, Iran*

(Dated: August 21, 2024)

Density functional theory has been applied to investigate structural and electronic properties of molybdenene monolayer in both its hexagonal and triclinic eigenstructures, within ultrasoft pseudopotential approach. In agreement with experimental findings, it has been found that either phase of molybdenene is metallic Dirac material, known as metallic relative of graphene. Partial density of state analysis has revealed that the  $d$  valence orbitals of molybdenum atoms have had the largest contribution to such a metallic property, due to being half-empty and being the outermost. Phonon-dispersion calculations also have led to negative frequencies or soft modes for both eigenstructures, showing their instability in terms of lattice dynamics, as reported in experimental literature.

**Keywords:** Molybdenene; Two-dimensional (2D); Nanoscale; Electronic structure; Density functional theory (DFT)

**PACS Numbers:** 71.15.Mb, 73.20.At, 73.22.-f, 63.20.Dj

## I. INTRODUCTION

Beginning with the landmark discovery of graphene [1, 2] about two decades ago, many areas of science and technology, from materials science [3] to electronics [4] to medicine [5], have experienced a prodigious revolution since then, making researchers passionately look for other possible low-dimensional materials with similar uniqueness, some paramount of which are two-dimensional (2D) MXenes such as MoS<sub>2</sub> [6] and WS<sub>2</sub> [7], phagraphene [8], borophene [9], SLSiN [10] (single-layer silicon nitride), fluorographenes [11, 12], graphene oxides [13], B<sub>2</sub>C graphene sheet [14], h-BN [15], Ti<sub>2</sub>C and Ti<sub>3</sub>C [16], and so on [17].

Characterized by massless quasi-particles in their low-energy excitation spectrum, Dirac materials [18] also fall into the category of low-dimensional nanoscale materials, which include  $d$ -wave superconductors [19], Weyl and Dirac semi-metals, graphene, topological insulators [20], and superfluid phases of <sup>3</sup>He [21], exhibiting a range of unique and universal properties: the same power-law temperature dependence of fermionic specific heat [18], response magnetic fields and impurities, transport properties, suppressed back-scattering, and optical conductivity [22].

In contrast to other kinds of 2D materials, elemental Dirac or Dirac-like materials—such as phosphorene [23], graphene, silicene [24], borophene, and 2D gold [25]—are of especial interest, for they typically lack structural impurities, leading to enhanced electron mobility as a result. Advancements in

discovery of low-dimensional and Dirac materials have further led to the inclusion of higher-atomic-number metallic atoms such as Mo, W, and Ti, the electronic densities of which have to be distributed only in two dimensions, resulting in potential exotic electronic and excitonic properties, which make them mechanically robust under high loads and temperatures [26] as a result.

As a common behavior, none of the Dirac materials identified has so far showed metallic properties. A recent investigation has experimentally confirmed the formation of free-standing molybdenene monolayer [27] as a 2D Dirac material with metallic properties nevertheless, purely composed of Mo atoms. According to the literature, during the production of molybdenene, weakly-bonded molybdenene sheets are first formed, which, later on, exhibit metallic properties upon exfoliation. This so-called molybdenene monolayer, with electrical conductivity of about 940 S.m<sup>-1</sup>, has also been reported to acquire tunable electronic and optical properties upon hybridization with 2D h-BN and MoS<sub>2</sub>.

Experimentally, two phases/eigenstructures have so far been identified at different areas of molybdenene monolayer, taking hexagonal and triclinic crystal structures, as illustrated in Fig. 1, being abbreviated here as HM (hexagonal molybdenene) and TM (triclinic molybdenene), respectively.

---

\* shekaari@email.kntu.ac.ir; shekaari.theory@gmail.com

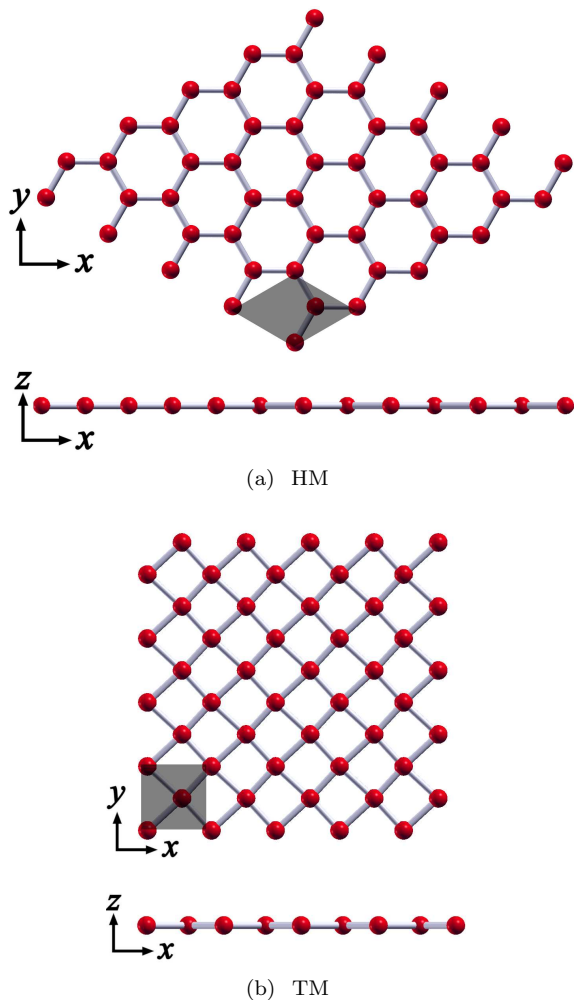


FIG. 1. The  $5 \times 5$  supercells of (a) HM and (b) TM in  $x-y$  and  $x-z$  planes, as well as their associated unit cells showed by gray areas—rendered in XCrySDen [28]. Either unit cell contains two Mo atoms.

The electronic structure of molybdenene monolayer has formerly been reported [27] within the framework of density functional theory (DFT) [29] and the projector-augmented-wave (PAW) method [30]. Nevertheless, we here have adopted a different approach based on ultrasoft pseudopotentials (USPP) [31] to investigate the metallic properties of both HM and TM eigenstructures, and demonstrate that similar results will be found.

The present work has been organized as follows: Sec. II describes computational details, Sec. III discusses the results calculated; and Sec. IV concludes our discussion.

## II. COMPUTATIONAL DETAILS

We have adopted the self-consistent [32], plane-wave, ultrasoft, pseudopotential approach of DFT,

at the PBE-GGA [33] level of approximation, as implemented in QUANTUM ESPRESSO integrated suite [34–36]. The running mode has been multi-core parallelized by Open MPI [37], on Linux (Debian) operating system [38, 39]. The scalar-relativistic, ultrasoft [40] pseudopotential file `Mo.pbe-spn-rrkjus_ps1.0.2.UPF` [41], generated by Rappe-Rabe-Kaxiras-Joannopoulos (RRKJ) [42] pseudization recipe with non-linear core correction [43], has been used to model the core electrons; the valence shell has also included  $4s^2 4p^6 5s^1 4d^5 5p^0$  orbitals according to that file. The electronic density has been augmented by means of a Fourier interpolation scheme in real space [44]. The kinetic energy cut-off values of about 1224 eV ( $\sim 90$  Rydberg) and 4900 eV ( $\sim 360$  Rydberg) have been found to be optimized for wavefunctions, and for the charge density and the potential, respectively. Two hexagonal (for HM) and triclinic (for TM) primitive cells have been used, each containing two Mo atoms (Fig. 1), under periodic boundary conditions, with optimized vacuum lengths of  $> 16$  Å along the  $z$ -axis to keep from periodic interactions.

To come up with reliable accuracy for phonon-dispersion calculations, a number of strict conditions have accordingly been adopted including: a self-consistency energy convergence threshold of about  $10^{-12}$  eV; a force convergence threshold of  $< 2.58 \times 10^{-5}$  eV.Å $^{-1}$  for ionic relaxation based on quasi-Newtonian Broyden-Fletcher-Goldfarb-Shanno (BFGS) geometry optimization method [45]; and a threshold of  $10^{-14}$  for phonon-dispersion self-consistency. The initial lattice constant for either eigenstructure has been set to 3.70 Å (namely, the experimental value reported for TM in the literature [27]); the final lattice constants and atomic positions have then been obtained via applying both variable-cell as well as fixed-cell relaxation simulations. The Brillouin zone samplings of HM and TM have been carried out along two close  $k$ -space paths  $\Gamma$ -M-K- $\Gamma$ , and  $\Gamma$ -X-M- $\Gamma$ , meshed by 151  $k$ -points, respectively; the smearing method has also been set to Methfessel-Paxton [46] method.

All the values/schemes reported/applied here have been determined/adopted optimally based on their associated energy-convergence tests. All the software packages used in the present work are also either free under or compatible with the GNU general public license (GPL) [47].

Theoretically, despite the present work is based on calculations at absolute zero ( $T = 0$ ), the obtained results (namely, the ground-state properties) are applicable to as much higher temperatures as room temperature, according to the fact that room temperature for the electron gas model at metallic densities is in

fact a very low temperature, indistinguishable from  $T = 0$  for many purposes [48].

### III. RESULTS

#### A. Structural properties

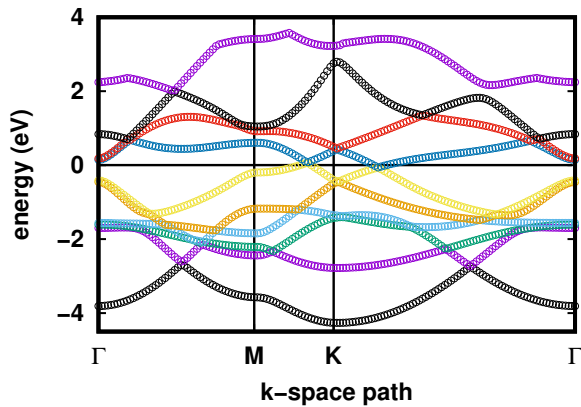
The final equilibrium lattice constants have been found about 4.05627 and 2.8471 Å for HM and TM, respectively. The Mo–Mo bond lengths after relaxation have also been 2.3416 Å for HM, and 2.2244 Å for TM. The relaxed atomic positions have been tabulated in Table. I.

TABLE I. Cartesian components of the atomic positions of HM and TM after relaxation.

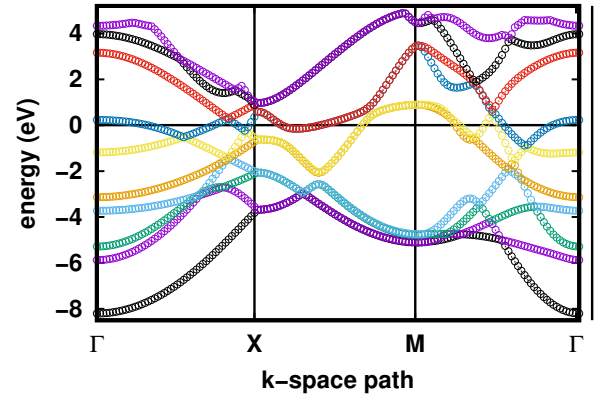
Eigenstructure	Atom	$x$ (Å)	$y$ (Å)	$z$ (Å)
HM	Mo	0.25470	0.14705	0.00000
	Mo	2.28256	1.31876	0.00000
TM	Mo	0.43451	-0.00019	0.00000
	Mo	1.85807	1.70907	0.00000

#### B. Electronic structure

Fig. 2 illustrates the electronic band structures of HM and TM.



(a) HM

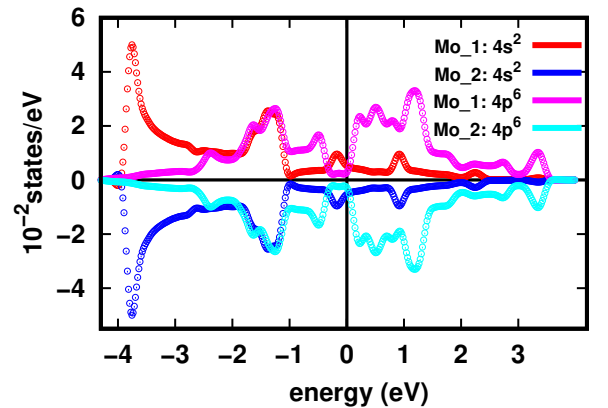


(b) TM

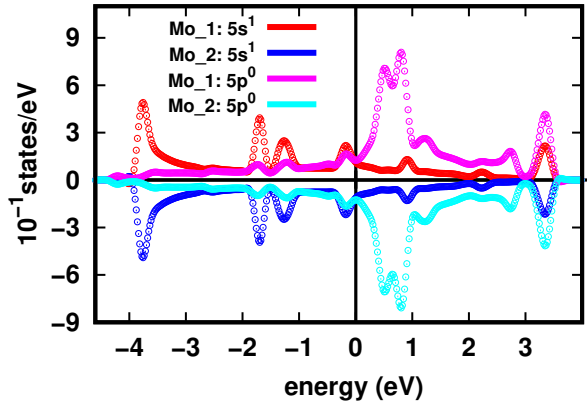
FIG. 2. Electronic band structures of (a) HM and (b) TM—rendered in Gnuplot [49]. The Fermi energy is zero of the diagrams, being crossed by the energy bands as a consequence of metallic feature.

As is seen, the energy bands cross the Fermi level (zero of the diagrams), indicating the metallic property of either eigenstructure, in agreement with the literature.

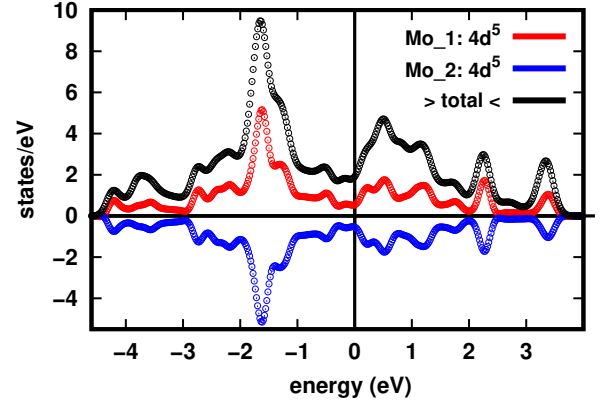
Electronic density of state (DOS) diagrams of Fig. 3 also confirm the same result, showing total DOS as well as partial contributions of the valence orbitals  $4s^2$ ,  $4p^6$ ,  $5s^1$ ,  $4d^5$ , and  $5p^0$ , for each atom of the unit cells. The following analyses are valid for both HM and TM monolayers.



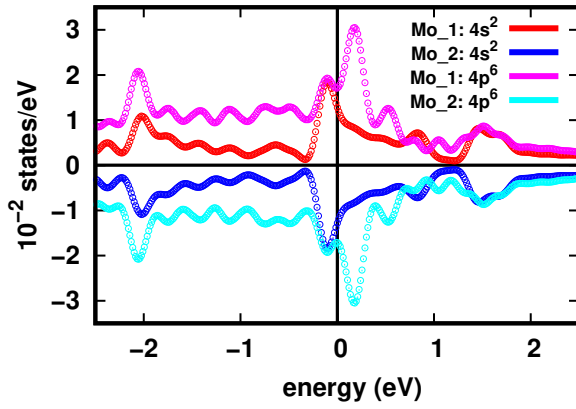
(a) HM



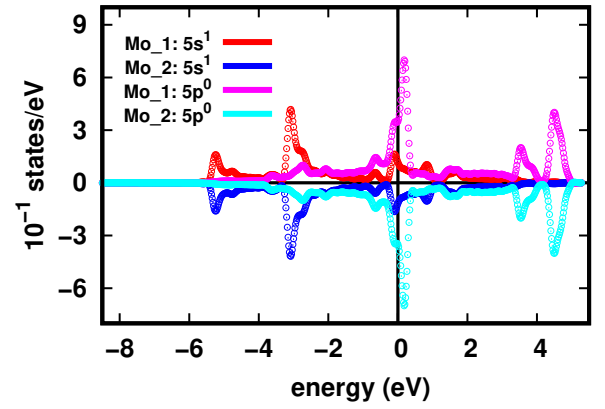
(b) HM



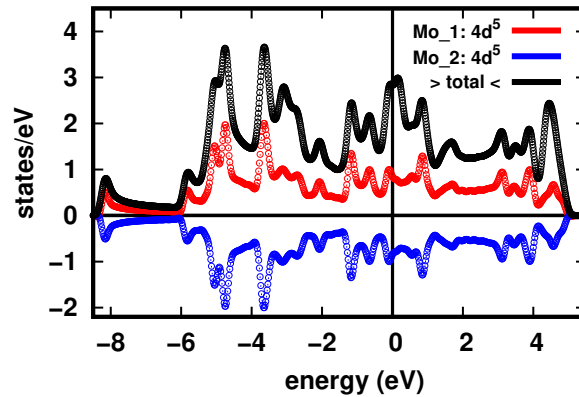
(c) HM



(d) TM



(e) TM



(f) TM

FIG. 3. Electronic DOS for HM [(a) to (c)] and TM [(d) to (f)], including total DOS (in black) as well as partial contributions of the valence orbitals  $4s^2$ ,  $4p^6$ ,  $5s^1$ ,  $4d^5$ , and  $5p^0$ , of both Mo atoms (labeled by \_1 and \_2) of the unit cells. The curves belonging to Mo\_2 have been flipped vertically to avoid confusion with those of Mo\_1. Zero of the diagrams is the Fermi level.

The metallic property of either monolayer is evident due to the Fermi level (zero of the diagrams) being crossed, consistent with band structure analysis. According to sub-figures, the orbitals can be classified in three sets in terms of their states/eV values, being different from each other, in ascending order, by one order of magnitude: (i)  $4s^2 4p^6$  in Figs. 3(a) and 3(d); (ii)  $5s^1 5p^0$  in Figs. 3(b) and 3(e); and (iii)  $4d^5$  in Figs. 3(c) and 3(f).

From Figs. 3(a) and 3(d), the orbitals  $4s^2$  and  $4p^6$  have the least contribution to electric conductivity based on the fact that these orbitals have no empty states; therefore according to Pauli's exclusion principle, electrons cannot enter/move within such full states.

According to Figs. 3(b) and 3(e), the orbitals  $5s^1$  and  $5p^0$  have larger contributions compared to set (i), based on the same reasoning: half of the former ( $5s^1$ ) and entire of the latter orbital ( $5p^0$ ) are empty, giving charge carriers within/adjacent to these orbitals the required kinetic degree of freedom to conduct electricity as well. Since electronic configuration of Mo is [Kr]  $5s^1 4d^5$ , the next orbital  $5p$  has accordingly no atomic electron (so,  $5p^0$ ); therefore, only conduction electrons can enter this orbital according to Drude's model [50].

The largest contributions to total DOS, according to Figs. 3(c) and 3(f), arise from  $4d^5$ , which are the outermost orbitals (accordingly contain weakest-bound atomic electrons) the halves of which are empty, leading to largest share in electric conductivity of either monolayer as a result. This is why the shapes of total DOS curves (black curves) are mainly determined by those orbitals.

### C. Lattice stability

To determine the lattice stability of either eigenstructure, we also have applied phonon-dispersion calculations at  $\Gamma$  point, with strict conditions on re-

lated convergence parameters as described in Sec. II. However, in agreement with experimental results of the literature, we have found soft modes (negative frequencies) at this point, whose values have been tabulated in Tab. II, showing that either monolayer is not stable in terms of lattice dynamics.

TABLE II. The frequency values associated to six modes of lattice vibration for HM and TM, computed during phonon-dispersion calculations.

Eigenstructure	Mode Number	Frequency (THz)
HM	1	-0.233318
	2	-0.127262
	3	0.352582
	4	7.822404
	5	8.959422
	6	10.969448
TM	1	-1.579797
	2	-0.394524
	3	-0.354504
	4	0.323400
	5	15.490007
	6	20.172375

## IV. CONCLUDING REMARKS

We have applied density functional theory within ultrasoft pseudopotential approach to inquire into structural and electronic properties of molybdenene monolayer in both its hexagonal and triclinic phases. In agreement with experimental findings, we have found that: (i) either phase/eigenstructure of molybdenene has showed metallic properties based on electronic band structure and density of states (DOS) analyses; (ii)  $4d^5$  valence orbitals of the Mo atoms of the unit cells have had the largest contribution to such a metallic feature due to being half-empty as well as being the outermost orbitals, according to partial DOS calculations; and (iii) either eigenstructure is unstable in terms of lattice dynamics, leading to negative frequencies / soft modes following phonon-dispersion calculations.

---

[1] K.S. Novoselov, A.K. Geim, S.V. Morozov, D. Jiang, Y. Zhang, S.V. Dubonos, I.V. Grigorieva, A.A. Firsov, Electric field effect in atomically thin carbon films, *Science* 306 (2004) 666.

[2] M.I. Katsnelson, K.S. Novoselov, Graphene: New bridge between condensed matter physics and quantum electrodynamics, *Solid State Commun.* 143 (2007) 3.

[3] X. Zhang, B.R.S. Rajaraman, H. Liub, S. Ramakrishna, Graphene's potential in materials science and engineering, *RSC Adv.* 4 (2014) 28987.

[4] 15 years of graphene electronics, *Nat. Electron.* 2 (2019) 369.

[5] K. Yang, L. Feng, X. Shi, Z. Liu, Nano-graphene in biomedicine: theranostic applications, *Chem. Soc. Rev.* 42 (2013) 530.

- [6] X. Li, H. Zhu, Two-dimensional MoS<sub>2</sub>: Properties, preparation, and applications, *J. Materiomics* 1 (2015) 33.
- [7] A. Klein, S. Tiefenbacher, V. Eyert, C. Pettenkofer, W. Jaegermann, Electronic properties of WS<sub>2</sub> mono-layer films, *Thin Solid Films* 380 (2000) 221.
- [8] Z. Wang, X.-F. Zhou, X. Zhang, Q. Zhu, H. Dong, M. Zhao, A.R. Oganov, Phagraphene: a low-energy graphene allotrope composed of 5-6-7 carbon rings with distorted Dirac cones, *Nano Lett.* 15 (2015) 6182.
- [9] A.J. Mannix, X.-F. Zhou, B. Kiraly, J.D. Wood, D. Alducin, B.D. Myers, X. Liu, B.L. Fisher, U. Santiago, J.R. Guest, M.J. Yacaman, A. Ponce, A.R. Oganov, M.C. Hersam, N.P. Guisinger, Synthesis of borophenes: Anisotropic, two-dimensional boron polymorphs, *Science* 350 (2015) 1513.
- [10] A. Shekaari, M. Jafari, Unveiling the first post-graphene member of silicon nitrides: A novel 2D material, *Comput. Mater. Sci.* 180 (2020) 109693.
- [11] A.N. Enyashin, A.L. Ivanovskii, Fluorographynes: Stability, structural and electronic properties, *Superlattices Microstruct.* 55 (2013) 75.
- [12] J. Sivek, O. Leenaerts, B. Partoens, F.M. Peeters, First-Principles Investigation of Bilayer Fluorographene, *J. Phys. Chem. C* 116 (2012) 19240.
- [13] D.R. Dreyer, S. Park, C.W. Bielawski, R.S. Ruoff, The chemistry of graphene oxide, *Chem. Soc. Rev.* 39 (2010) 228.
- [14] X. Wu, Y. Pei, X.C. Zeng, B<sub>2</sub>C Graphene, Nanotubes, and Nanoribbons, *Nano Lett.* 9 (2009) 1577.
- [15] S. Wang, Studies of Physical and Chemical Properties of Two-Dimensional Hexagonal Crystals by First-Principles Calculation, *J. Phys. Soc. Jpn.* 79 (2010) 064602.
- [16] A.N. Enyashin, A.L. Ivanovskii, Structural and Electronic Properties and Stability of MXenes Ti<sub>2</sub>C and Ti<sub>3</sub>C<sub>2</sub> Functionalized by Methoxy Groups, *J. Phys. Chem. C* 117 (2013) 13637.
- [17] Twenty years of 2D materials, *Nat. Phys.* 20 (2024) 1.
- [18] T.O. Wehling, A.M. Black-Schaffer, A.V. Balatsky, Dirac materials, *Adv. Phys.* 63 (2014) 1.
- [19] A.V. Balatsky, I. Vekhter, J.X. Zhu, Impurity-induced states in conventional and unconventional superconductors, *Rev. Mod. Phys.* 78 (2006) 373.
- [20] M.Z. Hasan, C.L. Kane, Colloquium: Topological insulators, *Rev. Mod. Phys.* 82 (2010) 3045.
- [21] G.E. Volovik, Exotic properties of superfluid <sup>3</sup>He, World Scientific, Singapore, 1992.
- [22] S. Das Sarma, S. Adam, E.H. Hwang, E. Rossi, Electronic transport in two-dimensional graphene, *Rev. Mod. Phys.* 83 (2011), 407.
- [23] H. Liu, A.T. Neal, Z. Zhu, Z. Luo, X. Xu, D. Tománek, P.D. Ye, Phosphorene: An Unexplored 2D Semiconductor with a High Hole Mobility, *ACS Nano* 8 (2014) 4033.
- [24] H. Oughaddou, H. Enriquez, M.R. Tchalala, H. Yildirim, A.J. Mayne, A. Bendounan, G. Dujardin, M. Ait Ali, A. Kara, Silicene, a promising new 2D material, *Prog. Surf. Sci.* 90 (2015) 46.
- [25] L. Wang, Y. Zhu, J.-Q. Wang, F. Liu, J. Huang, X. Meng, J.-M. Basset, Y. Han, F.-S. Xiao, Two-dimensional gold nanostructures with high activity for selective oxidation of carbon–hydrogen bonds, *Nat. Commun.* 6 (2015) 6957.
- [26] D.R. Lide, Handbook of Chemistry and Physics, 74th edition, CRC Press, 1993.
- [27] T.K. Sahu, N. Kumar, S. Chahal, R. Jana, S. Paul, M. Mukherjee, A.H. Tavabi, A. Datta, R.E. Dunin-Borkowski, I. Valov, A. Nayak, P. Kumar, Microwave synthesis of molybdenene from MoS<sub>2</sub>, *Nat. Nanotechnol.* 18 (2023) 1430.
- [28] A. Kokalj, XCrySDen—a new program for displaying crystalline structures and electron densities, *J. Mol. Graphics Modelling* 17 (1999) 176.
- [29] R.G. Parr, W. Yang, Density-Functional Theory of Atoms and Molecules, Oxford University Press, New York, 1989.
- [30] P.E. Blöchl, Projector augmented-wave method, *Phys. Rev. B* 50 (1994) 17953.
- [31] W.E. Pickett, Pseudopotential methods in condensed matter applications, *Comput. Phys. Rep.* 9 (1989) 115.
- [32] W. Kohn, L.J. Sham, Self-consistent equations including exchange and correlation effects, *Phys. Rev.* 140 (1965) A1133.
- [33] J.P. Perdew, K. Burke, M. Ernzerhof, Generalized gradient approximation made simple, *Phys. Rev. Lett.* 77 (1996) 3865.
- [34] P. Giannozzi, S. Baroni, N. Bonini, M. Calandra, R. Car, C. Cavazzoni, D. Ceresoli, G.L. Chiarotti, M. Cococcioni, I. Dabo, A.D. Corso, S. de Gironcoli, S. Fabris, G. Fratesi, R. Gebauer, U. Gerstmann, C. Gougoussis, A. Kokalj, M. Lazzeri, L. Martin-Samos, N. Marzari, F. Mauri, R. Mazzarello, S. Paolini, A. Pasquarello, L. Paulatto, C. Sbraccia, S. Scandolo, G. Sclauzero, A.P. Seitsonen, A. Smogunov, P. Umari, R.M. Wentzcovitch, QUANTUM ESPRESSO: a modular and open-source software project for quantum simulations of materials, *J. Phys.: Cond. Matter* 21 (2009) 395502.
- [35] P. Giannozzi, O. Andreussi, T. Brumme, O. Bunau, M. Buongiorno Nardelli, M. Calandra, R. Car, C. Cavazzoni, D. Ceresoli, M. Cococcioni, N. Colonna, I. Carnimeo, A. Dal Corso, S. de Gironcoli, P. Delugas, R.A. DiStasio Jr, A. Ferretti, A. Floris, G. Fratesi, G. Fugallo, R. Gebauer, U. Gerstmann, F. Giustino, T. Gorni, J. Jia, M. Kawamura, H.-Y. Ko, A Kokalj, E Küçükbenli, M. Lazzeri, M. Marsili, N. Marzari, F. Mauri, N.L. Nguyen, H.-V. Nguyen, A. Otero-de-la-Roza, L. Paulatto, S. Poncé, D. Rocca, R. Sabatini, B. Santra, M. Schlipf, A.P. Seitsonen, A. Smogunov, I. Timrov, T. Thonhauser, P. Umari, N. Vast, X. Wu, S. Baroni, Advanced capabilities for materials modelling with Quantum ESPRESSO, *J. Phys.: Condens. Matter* 29 (2017) 465901.
- [36] P. Giannozzi, O. Baseggio, P. Bonfá, D. Brunato, R. Car, I. Carnimeo, C. Cavazzoni, S. de Gironcoli, P. Delugas, F. Ferrari Ruffino, A. Ferretti, N. Marzari, I. Timrov, A. Urru, S. Baroni, Quantum ESPRESSO toward the exascale, *J. Chem. Phys.* 152 (2020) 154105.
- [37] <https://www.open-mpi.org>.
- [38] <https://www.debian.org>.
- [39] L. Torvalds, The Linux edge, *Commun. ACM* 42 (1999) 38.
- [40] D. Vanderbilt, Soft self-consistent pseudopotentials in a generalized eigenvalue formalism, *Phys. Rev. B* 41 (1990) 7892.
- [41] <https://www.quantum-espresso.org>

- [42] A.M. Rappe, K.M. Rabe, E. Kaxiras, J.D. Joannopoulos, Optimized pseudopotentials, *Phys. Rev. B* 41 (1990) 1227.
- [43] S.G. Louie, S. Froyen, M.L. Cohen, Nonlinear ionic pseudopotentials in spin-density-functional calculations, *Phys. Rev. B* 26 (1982) 1738.
- [44] P. Giannozzi, F. De Angelis, R. Car, First-principle molecular dynamics with ultrasoft pseudopotentials: Parallel implementation and application to extended bioinorganic systems, *J. Chem. Phys.* 120 (2004) 5903.
- [45] R. Fletcher, *Practical Methods of Optimization*, 2nd ed., New York: John Wiley & Sons, 1987.
- [46] M. Methfessel, A.T. Paxton, High-precision sampling for Brillouin-zone integration in metals, *Phys. Rev. B* 40 (1989) 3616.
- [47] <https://www.gnu.org/licenses/gpl-3.0.html>.
- [48] N.W. Ashcroft, N.D. Mermin, *Solid State Physics*, Cengage Learning, 1976.
- [49] <http://www.gnuplot.info>.
- [50] P. Drude, Zur Elektronentheorie der Metalle; II. Teil. Galvanomagnetische und thermomagnetische Effecte, *Ann. Phys.* 308 (1900) 369.